IEEE Transactions on Robotics (T-RO) paper, presented at ICRA 2026, Vienna, Austria. Cite as T-RO paper.

Frictional and Prismatic Pin-Array Gripper for Universal Gripping and Stable Tool Manipulation

Cheonghwa Lee, Hyeongwon Kim, Midum Oh, Kisu Ok, and Sung-Hoon Ahn

***Abstract*—Global trend in robotics has shifted toward deploying humanoid robots and mobile manipulators in industrial settings to automate repetitive and structured tasks traditionally performed by human workers. However, most tools and equipment are designed for human hands, and current grippers or end-effectors are highly specialized, limiting their ability to fully replace human handling of simple tools and tasks. This study proposes a novel frictional and prismatic pin-array gripper developed for universal gripping and tool manipulation. A pin-array structure of the gripper mimics the behavior of soft grippers while incorporating rigid components, enabling adaptability to various shapes and sizes. Each pin features semiautomatic actuation through a compression spring, supporting the underactuated mechanism. Most existing studies on grippers focus on simple pick-and-place tasks, whereas the proposed gripper extends functionality to practical tool usage. Enabled by the pin-array structure, it provides increased contact surface and support points, ensuring stable gripping and enhanced manipulation performance. In the evaluation, the pin-array gripper achieved a payload capacity of 2400 g, significantly outperforming the conventional RG2-FT gripper and the frictional flat gripper, which reached maximum capacities of 800 and 400 g, respectively. It also exhibited higher grasping forces, measuring 1.17 times greater than the RG2-FT gripper and up to 23 times greater than the frictional flat gripper. For tool manipulation, the pin-array gripper exhibited significantly lower manipulation errors, with 21.67 and 6.59 times fewer errors than the RG2-FT and flat grippers, respectively, when handling the hammer, and 7.69 and 4.45 times fewer for the metal file. In addition, qualitative demonstrations in universal gripping, omnidirectional gripping, and tool usage further validated the gripper's performance in mobile manipulator tasks.**

***Index Terms*—Grasping force, mobile manipulator, omnidirectional gripping, pin-array gripper, tool manipulation, universal gripping.**

I. Introduction

As THE demand for automation in industrial sectors increases, mobile manipulators and humanoid robots are rapidly expanding to replace repetitive tasks traditionally performed by human workers. Robots such as Atlas and Spot Boston Dynamics, Optimus Tesla, and Go2 and G1 Unitree are designed to handle a wide range of tasks, including pick-and-place, manipulation, inspection, and assembly, which typically require the use of specific tools.

However, most tools and equipment are designed for human hands, and current grippers or end-effectors are highly specialized for certain tasks, limiting their ability to fully replace human handling. When dealing with objects of various shapes, textures, weights, and material compositions, existing grippers often struggle to provide stable handling [1], [2], [3], [4]. While most gripper research has primarily concentrated on pick-and-place operations rather than tool utilization, the real need lies in enabling universal gripping and tool usage, making research in this area crucial for advancing robotic capabilities.

The main characteristic of the human hand is its multiple joints, which provide a high degree of freedom (DOF), enabling stable tool gripping and dynamic manipulation. However, in systems with high DOF, it becomes complex to manufacture, implement, and control each DOF. In addition, considerations such as path planning for oriented object gripping are crucial. To simplify this complexity, it is essential to focus on designing efficient grippers that utilize low DOF systems, which can effectively overcome these challenges while maintaining performance.

Grippers are broadly classified into two types: soft grippers and rigid grippers. Soft grippers, typically made from compliant materials like silicone, conform to object surfaces and excel at handling delicate or irregularly shaped items. Recent advancements incorporate rigid or hybrid components to achieve continuum-like deformation through structural or kinematic mechanisms [5], [6], [7], [8]. Their adaptability, relying on material deformation and friction, suits a range of applications but limits durability and load capacity, which hinders performance in precise or repetitive tasks. Examples of soft grippers include

Received 6 May 2025; revised 28 September 2025; accepted 11 October 2025. Date of publication 28 October 2025; date of current version 1 December 2025. This work was supported in part by the Ministry of Trade, Industry & Energy (MOTIE, Korea) through the Industrial Technology Innovation Program under Grant RS-2024-00507783, "The development of AI-based predictive maintenance and mobile autonomous robots for high-risk tasks in steel manufacturing processes" and in part by the National Research Foundation of Korea (NRF), through the Korea government, MSIT under Grant RS-2024-00356951. This article was recommended for publication by Associate Editor C. Della Santina and Editor M. Yim upon evaluation of the reviewers' comments. *(Cheonghwa Lee and Hyeongwon Kim contributed equally to this work.) (Corresponding author: Sung-Hoon Ahn.)*

Cheonghwa Lee is with the Department of the Electrical and Computer Engineering, Seoul National University, Seoul 08826, South Korea, and also with the School of Mechanical Engineering, Kumoh National Institute of Technology, Gumi 39177, South Korea (e-mail: haya.c.lee@kumoh.ac.kr).

Hyeongwon Kim and Midum Oh are with the Department of Mechanical Engineering, Seoul National University, Seoul 08826, South Korea (e-mail: alstk1956@snu.ac.kr; midumoh@snu.ac.kr).

Kisu Ok is with the Department of Electrical and Computer Engineering, Seoul National University, Seoul 08826, South Korea (e-mail: ksokngu@snu.ac.kr).

Sung-Hoon Ahn is with the Department of Mechanical Engineering, Seoul National University, Seoul 08826, South Korea, and also with the Institute of Advanced Machines and Design, Seoul National University, Seoul 08826, South Korea (e-mail: ahnsh@snu.ac.kr).

This article has supplementary downloadable material available at https://doi.org/10.1109/TRO.2025.3626656, provided by the authors.

Digital Object Identifier 10.1109/TRO.2025.3626656

the jamming gripper [7] and gecko-inspired adhesive grippers [9], both capable of handling complex geometries through flexible contact mechanisms [10]. However, these designs often face durability and payload limitations, which makes them less suitable for heavy-duty and precision tasks. The use of flexible materials in soft grippers also makes fabrication challenging, resulting in inconsistent manufacturing quality. In addition, soft grippers may struggle with distributing forces evenly, particularly on asymmetrical or irregularly shaped objects, leading to stability issues during manipulation. This imbalance not only impacts control performance but can also reduce the gripper's lifespan, as uneven force distribution may lead to premature wear or failure.

In contrast, rigid grippers, typically made from metals or hard plastics, provide high precision and strength, ideal for industrial applications involving heavy objects and fine assembly [3], [11], [12], [13]. Their consistent, linear contact enables stable grips on regular shapes, though they often struggle with irregular objects. Rigid grippers, such as the Shape Adaptive Lateral Stiffness Gripper [12] and Eclipse Pin-array Gripper [13] use mechanisms, such as parallel jaws [14] and adaptive pin-arrays [15] to improve contact and grip stability. However, the rigid structure of these grippers limits their adaptability to irregularly shaped or asymmetrical objects, reducing their flexibility in dynamic or unstructured environments. In addition, they tend to concentrate force at specific points, potentially damaging delicate objects due to their inability to conform to the surface.

To bridge these gaps, pin-array grippers offer a promising solution by combining adaptability with durability. These grippers use an array of pins to conform to an object's shape, increasing the contact point and enhancing grip stability. Pin-array grippers are generally categorized into 1) top–down press grippers [13], [16], which conform to topographical variations and (2) side press grippers [17], which stabilize objects from multiple sides. While top–down press pin-arrays excel at surface conformity, they are limited by the need for a supporting surface, which restricts their use in universal gripping applications [18], [19]. In addition, due to the gravitational force, objects can fall under certain conditions, raising safety concerns. On the other hand, side press grippers provide a more balanced grip, making them advantageous for irregularly shaped objects that require multidirectional support. A detailed comparison of these configurations is provided in Section II.

This study introduces a novel pin-array gripper that combines the flexibility of soft grippers with the robustness of rigid components, enabling adaptability to various shapes and sizes. The gripper's multiple contact points ensure a secure grip, which is crucial for stable manipulation and precise control, especially on complex or uneven surfaces. This stability is particularly valuable in applications requiring high accuracy, such as assembly lines [20] and precision-based tasks [21], where it minimizes errors and enhances overall task reliability. The frictional fingertips prevent slippage on smooth or slippery surfaces, allowing secure handling of various materials [22]. The nonslip fingertips are especially beneficial in applications involving delicate or valuable items, ensuring safe, stable handling throughout manipulation [23], [24]. The nondirectional pin-array design enables seamless adaptation to irregular shapes and surfaces. Each pin moves independently, conforming accurately to diverse object contours without prior knowledge of shape or orientation, making it particularly effective in unpredictable, unstructured environments, such as waste sorting, archaeological excavation, and industrial applications [20], [25], [26], [27]. Structural and force distribution analyses were conducted to verify the gripper's performance. Experiments are conducted to evaluate payload capacity, grasping force, and dynamic tool manipulation, along with a quantitative comparison against conventional grippers. In addition, qualitative evaluations are performed through universal gripping, omnidirectional tool gripping, tool usage, and application in the mobile manipulator LeeAhn2.

The main contributions of the proposed pin-array gripper for universal gripping and stable tool manipulation, as illustrated in Fig. 1, are as follows.

1) *Double-Sided Pin-Array Mechanism*: The proposed mechanism utilizes a pin-array that adapts to the shape of objects and provides support from both sides, offering a more balanced and secure hold as shown in Fig. 1(a).
2) *Multiple contact points and nonslip frictional fingertip*: The gripper's conformable pin-array provides multiple contact points by adjusting to the shape of objects, as shown in Fig. 1(b). The gripper incorporates nonslip frictional elements at the pin tips, increasing friction between the gripper and the object.
3) *Omnidirectional tool gripping:* The omnidirectional capability, illustrated in Fig. 1(c), allows the gripper to approach and secure objects from any direction.

These contributions advance robotic gripper technology and address practical automation challenges by offering adaptable, efficient, and easily integrable solutions. Our work has the potential to introduce new functionalities and enhance the productivity and versatility of automated systems.

II. Related Work on Pin-Array Gripper

This section presents a comparative analysis of the proposed pin-array gripper and existing pin-array grippers with similar designs and functionalities. We review four existing side press pin-array design and operation mechanisms, discussing their strengths, limitations, and comparison with the proposed pin-array gripper.

Ince et al. [28] proposed a form-flexible pin gripper with a 7×5 array of metal pins, each capable of axial movement. The pneumatic system allows the pins to conform to the object's shape for gripping, with compressed air securing the object and vacuum pressure releasing it. While the system is adaptable for high-temperature parts, it suffers from added pneumatic complexity, bulky mechanical structure, and limited compatibility with nonmetallic objects. This system is not suitable for tool manipulation.

Hasan et al. [17] proposed a hyper-adaptive robotic gripper with a thumb mechanism featuring a 5×12 pin-array of 60 steel pins that adapt to various object shapes. Each pin has a friction-enhancing tip and is restored by a spring structure. The finger, with a dual-joint spring structure, operates with two motors.

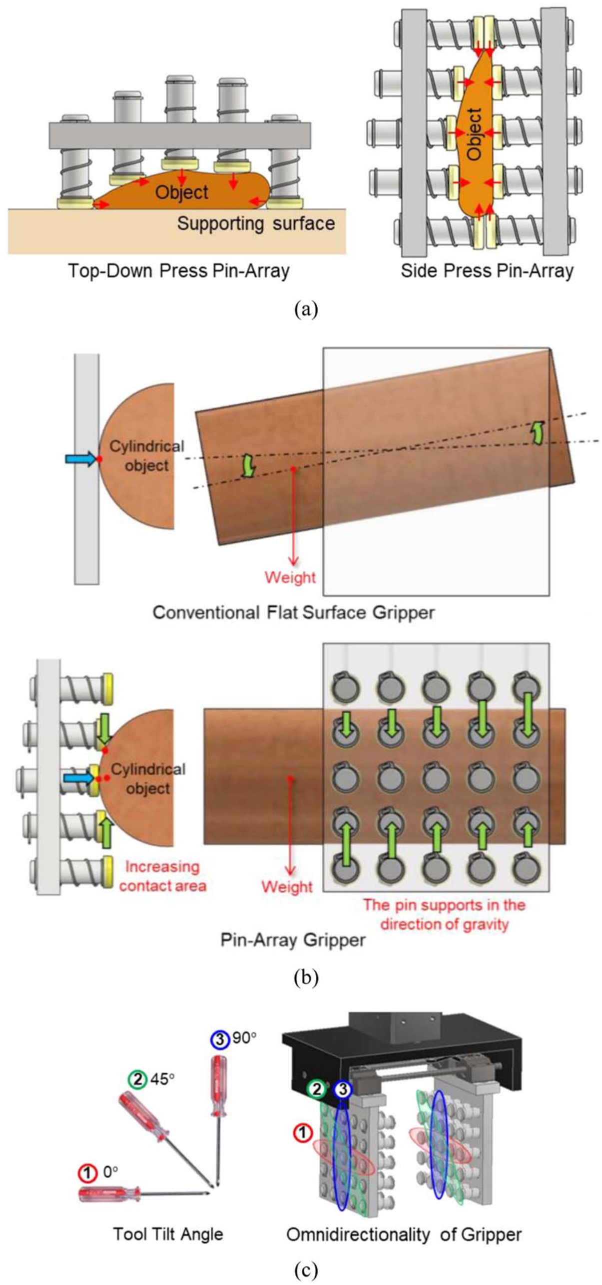

Fig. 1. Academic contribution of the proposed pin-array gripper. (a) Comparison of pin-array mechanism. (b) Comparison of contact area. (c) Omnidirectional tool gripping.

However, the silicone spring raises durability concerns, and the use of multiple motors increases complexity. The design is not suitable for tool manipulation tasks.

Flintoff et al. [29] proposed a hyper-adaptive robotic hand with finger pads made of rubber and steel pins arranged in 4 $\times$ 3 and 4 $\times$ 4 arrays. These pins, inserted into deformable silicone molds, passively conform to objects of various shapes and are supported by an articulated structure. The hand is actuated by two Dynamixel MX-64AR motors using tendons, but the design has limitations, including insufficient pin length for small objects and increased friction due to rotational motion. The maximum grasping force per pin is 1.2 N, and the maximum force per finger is 60 N. The design is not intended for tool manipulation, although the hyper-adaptive pad structure allows potential for such applications.

Tanaka et al. [30] proposed the GOAT gripper, a rigid underactuated gripper based on a whippletree mechanism that distributes force across two fingers using a single linear dc actuator. It features a spring-rod pin-array with micro-spines for a secure grip on irregular surfaces. The gripper adapts passively to objects with high friction but can damage objects during gripping. Its design simplifies the environment based on a minimum bounding box, reducing performance with irregular objects. The gripper is not intended for tool manipulation but for gripping structures in unstructured environments like wall climbing.

In comparison to the gripper presented in the study, our proposed design is specifically intended for tool manipulation and operates with a single motor, thereby simplifying the actuation mechanism. Unlike the gripper that relies on more complex actuation methods, such as tendons or pneumatic pressure, our design functions efficiently with a prismatic structure. Furthermore, the gripper is engineered to handle objects delicately, ensuring that no damage is inflicted on the gripped objects during manipulation, thus enhancing its applicability in sensitive tasks. The use of 3D-printed pins enhances maintenance by making them easy to replace and reduce production costs.

III. Pin-Array Design and Actuation Mechanism

This section details the design and assembly of the pin-array gripper and explains how the gripping works.

A. Design and Assembly of Pin-Array Gripper

The overall design of the pin-array gripper is shown in Fig. 2(a), which is divided into two main parts: 1) an actuation part and 2) a pin-array part. The actuation part moves two array plates to control the opening and closing motion of the gripper, consisting of a gripping motor, connecting rods, linear bushings, and linear shafts. The gripping motor, serving as the actuation source, is a Dynamixel XL-430 by Robotis. The connecting rod, 3D printed from acrylonitrile butadiene styrene (ABS) material, transfers the actuation from the gripping motor to the linear bushing. The linear bushing (SMA3GUU) guides linear motion with an inner diameter of 3 mm, while the linear shaft (E-PSFJ3-100) has a diameter of 3 mm and a length of 100 mm.

The pin-array part consists of two pin-array sets, each containing a 50 mm $\times$ 50 mm square array plate with 25 pin assemblies. Each array plate is made of aluminum and contains 25 holes arranged in a 5 $\times$ 5 configuration, with a uniform 10 mm spacing between holes in both the row and column directions. Each pin assembly consists of a fingertip, a pin, a compression spring, and a snap ring, as shown in Fig. 2(b). The pin assemblies are arranged in the array plate according to the hole pattern. The fingertips are made of soft, flexible resin, enhancing friction between the target object and the pin assembly to provide a secure grip. The pin has a cylindrical shape with flanges and is manufactured using ABS plastic on a 3D printer. The flange has an outer diameter of 6.5 mm, the main body has a diameter of 5 mm, and the snap ring insertion groove has a diameter

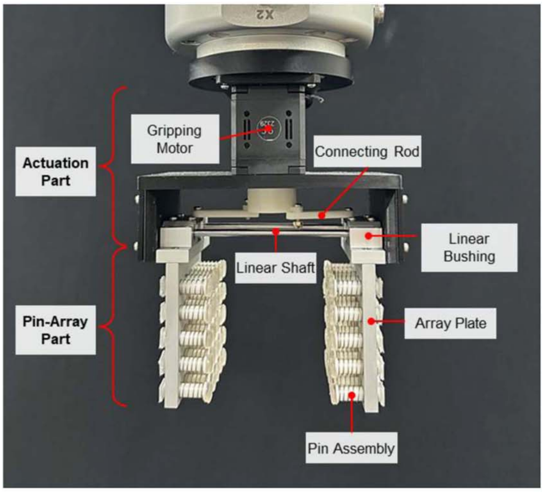

(a)

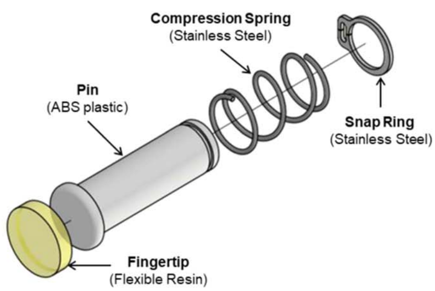

(b)

Fig. 2. Design of pin-array gripper. (a) Front view and components of the gripper. (b) Detail design of pin assembly.

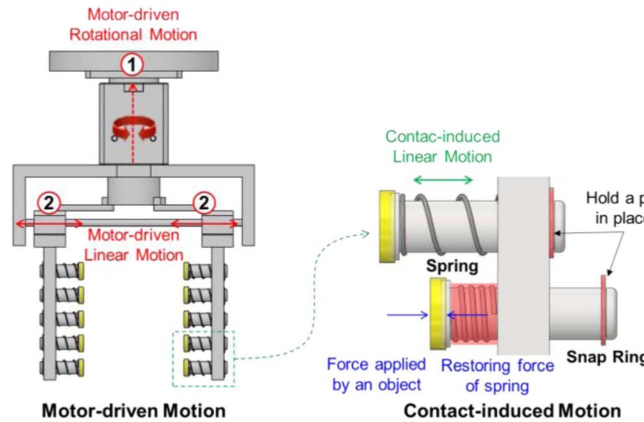

Fig. 3. Actuation mechanism of pin-array gripper.

of 4.5 mm. The total length of the pin is 17 mm from end to end. The compression spring has an outer diameter of 6 mm, a length of 10 mm, and a wire diameter of 0.4 mm. It passively holds the object in place through its repulsive force when the pin is compressed by the object. The snap ring, located at the pin groove, functions to secure the pin in place when it returns to its original position.

The overall dimensions of the gripper are 100 mm in length, 60.25 mm in width, and 89.5 mm in height, with a weight of 231.2 gm. It provides an operating workspace of 50 mm by 50 mm by 50 mm. The gripper operates at a linear velocity of 15 mm/s and has a maximum payload capacity of 2400 gm.

B. Gripping Mechanism

The pin-array gripper performs two types of motion, as shown in Fig. 3: 1) motor-driven motion, initiated by command input and governed by a simple threshold-based torque feedback control and 2) contact-induced motion, which passively responds to external forces through spring compression when a pin contacts an object surface. Motor-driven motion allows for control of the command signal, enabling the gripping motor to rotate, as illustrated on the left side of Fig. 3. This rotation drives a connecting rod linked to the array plates, which then move along the linear guide, effectively transforming the rotational actuation into linear motion. This linear motion constricts the parallel plates, enabling the gripper to enclose and hold the target object. The gripper employs a simple feedback control algorithm, where a torque threshold causes the motor to stop, adjusting the array plates based on the size of the object to be gripped. During the grasping process, the motor load gradually increased until it reached a preset threshold, at which point the motion stopped. In our experiments, the load threshold was set to 4 kgf.

Contact-induced motion, in contrast, is driven by an external force acting on a compression spring [27], [31], as illustrated on the right side of Fig. 3. When a pin contacts the surface of an object, it is pressed inward, and the spring provides a repulsive force to hold the object securely. This mechanism allows each pin to adapt individually to the contour of the object, ensuring an effective grip even on irregularly shaped surfaces. The snap ring at the end of each pin constrains its position, ensuring the pin returns to its original state once the object is released. This passive adaptation enables the gripper to conform to the target object without requiring complex sensors or additional actuators [32], [33]. When an object applies force to the pins, the spring compresses, and the restoring force from the snap ring maintains stability, supporting consistent gripping performance and structural integrity.

IV. Pin-Array Parameter and Structural Analysis

This section analyzes the structure and load characteristics of the pin-array gripper based on various parameters. In this article, we employ only one synthesis of each parameter. These analyses assist in optimizing the performance of pin-array grippers and enhancing their design for various applications.

A. Parametric Structure Analysis

In the parametric structure analysis, parameters are divided into pin-related parameters and array-related parameters as shown in Fig. 4(a). Pin-related parameters include the pin shape, radius r, and length l of the pins. Array-related parameters include the density between pins, as well as the lengths w and height h between pins along the X- and Y-axis in a two-dimensional configuration, and the thickness t along the Z-axis.

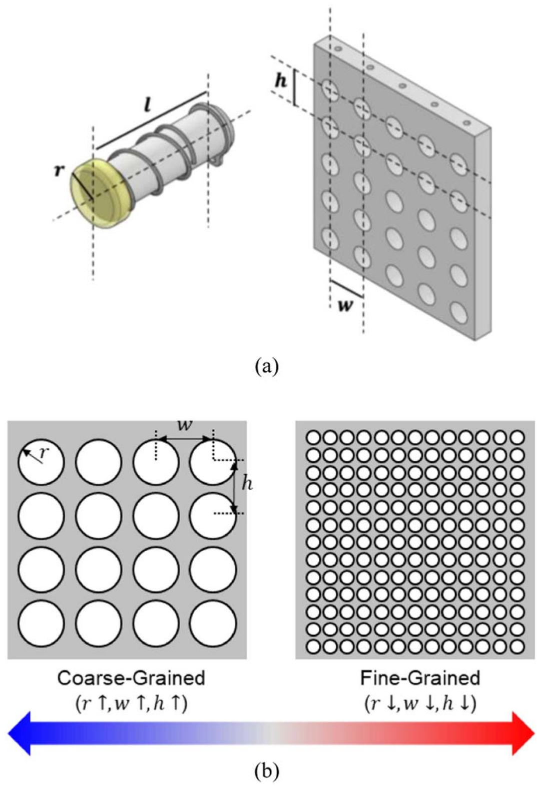

Fig. 4. Parametric structure analysis. (a) Parameters of pin and array. (b) Granularity of pin-array structure.

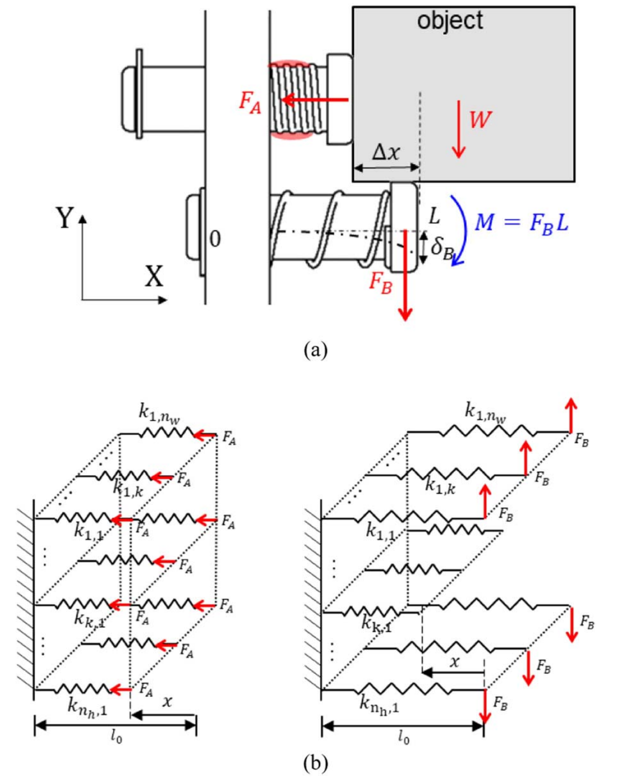

Fig. 5. Parametric load analysis. (a) Two types of force. (b) Parallel force analysis.

The pin has a radius r of 2.5 mm, and the length l of the pin is 17 mm from end to end. The plate has lengths w and h of 10 mm. The pin used in the gripper mechanism has a radius r of 2.5 mm and a total length l of 17 mm from end to end. The corresponding plate has a width w and height h of 10 mm.

The granularity of a pin-array gripper, as shown in Fig. 4(b), defined by the size and spacing of pins, significantly affects the contact surface area and gripping performance. Coarse granularity uses larger, more widely spaced pins, which reduces the overall contact surface area but provides a concentrated gripping force. This setup is well-suited for simpler, larger objects where fine adaptability is less critical. With fewer contact points, coarse-granularity designs also simplify control and reduce effort for maintenance, making them ideal for tasks with lower precision demands. In contrast, fine granularity employs smaller, closely spaced pins that expand the contact surface area, allowing the gripper to closely conform to complex or delicate object shapes. This increased contact surface distributes forces more evenly, enhancing stability and precision, which is particularly beneficial in applications requiring high accuracy.

The effectiveness of a pin-array gripper can be further tailored by adjusting design parameters, such as pin size, spacing, and array configuration. For instance, fine-grained configurations offer better control and handling of delicate objects, while coarser designs support robust handling of heavier items. This customization capability allows the gripper to be optimized for specific industrial applications, ensuring efficiency and stability across a range of gripping tasks.

B. Parametric Load Analysis

Each pin experiences two types of forces: 1) axial force and 2) bending force, as illustrated in Fig. 5(a).

For the axial force F_A, Hooke's Law is applied

$$F_A = -k\Delta x \tag{1}$$

where k (N/m) is the rated spring constant (stiffness), and Δx (mm) is the displacement from the original position. The spring has a constant of 0.4 N/mm.

For the bending force, which induces a moment on the pin, we calculate the moment M as

$$M = -F_B L \tag{2}$$

where F_B represent the bending force, and L is the distance from the base of the pin to the point of force application. In this context, F_B is derived from the total weight W of the object being gripped, which is assumed to be uniformly distributed across all contacting pins

$$F_B = \frac{W}{n} \tag{3}$$

where n is the number of pins in contact. The resulting bending deformation δ_B is described by

$$\delta_B = \frac{F_B L^3}{3EI} \tag{4}$$

where I is the area moment of inertia, which quantifies the pin's resistance to bending. The second moment of area I for a cantilever beam with a solid circular cross-section with radius r is given by

$$I = \frac{\pi r^4}{4}. \tag{5}$$

The 2D array structure, shown in Fig. 5(b), forms the basis of the net force of the pin-array gripper, which is calculated through the parallel summation of individual forces

$$F_{Net} = \sum F_A + \sum F_B \tag{6}$$

where F_A and F_B represent forces from different components within the array. This setup enables the gripper to achieve a combined force by summing the contributions of each element in parallel, with the total force being proportional to the number of pins in the width direction (n_w) and the number of pins in the height direction (n_h). Such a configuration enhances the ability of the gripper to maintain a stable and secure grip across various surfaces, distributing force evenly and thus improving overall gripping efficiency and effectiveness.

The analyses conducted are fundamental for designing compression and tension springs, as it allows engineers to predict stiffness and deformation resistance under load. The wire diameter directly influences stiffness, with larger diameters providing increased rigidity. The spring constant dictates the force needed to compress each pin, and connecting multiple springs in parallel proportionally enhances the total force. Thus, using thicker or stiffer pins improves stability for heavier objects, while smaller, more flexible pins allow for higher array density and adaptability to diverse shapes.

V. Experimental Evaluation

This section quantitatively evaluates the performance of the pin-array gripper through a series of experiments focused on payload capacity, grasping force, and dynamic tool manipulation. Each experiment was benchmarked against the commercial RG2-FT gripper (OnRobot) as well as the nonfrictional and frictional flat grippers.

The nonfrictional and frictional flat grippers were designed to share the same structural framework as the pin-array gripper to ensure consistency in material properties and geometric configuration. The nonfrictional flat gripper was constructed by 3D printing a 10.5 mm thick polylactic acid plate, which was then mounted onto the array plate structure used in the pin-array gripper. The frictional flat gripper incorporated 1 mm thick Flexible 80A resin fingertips and assembled onto the nonfrictional flat gripper, resulting in a total thickness of 11.5 mm.

A. Payload Measurement

The payload capacity of the gripper is a critical metric for evaluating gripping performance, particularly for pick-and-place tasks. This capacity is directly influenced by surface friction and grasping force, both of which must be sufficient to prevent slippage during handling.

To assess payload capacity, a weight-based measurement procedure was employed. The experimental setup, illustrated in Fig. 6, includes two distinct configurations tailored to different payload ranges. The first configuration [see Fig. 6(a)] was used to evaluate low payload capacities ranging from 100 to 1000 g in 100 g increments, whereas the second configuration [see Fig. 6(b)] was designed for heavier loads ranging from 1500 to 2500 g, also in 100 g increments. In both setups, cube-shaped objects were rigidly mounted to ensure consistent and reliable measurement of payload capacity. Four grippers were tested for comparison: the commercial RG2-FT gripper, the nonfrictional flat gripper, the frictional flat gripper, and the proposed pin-array gripper.

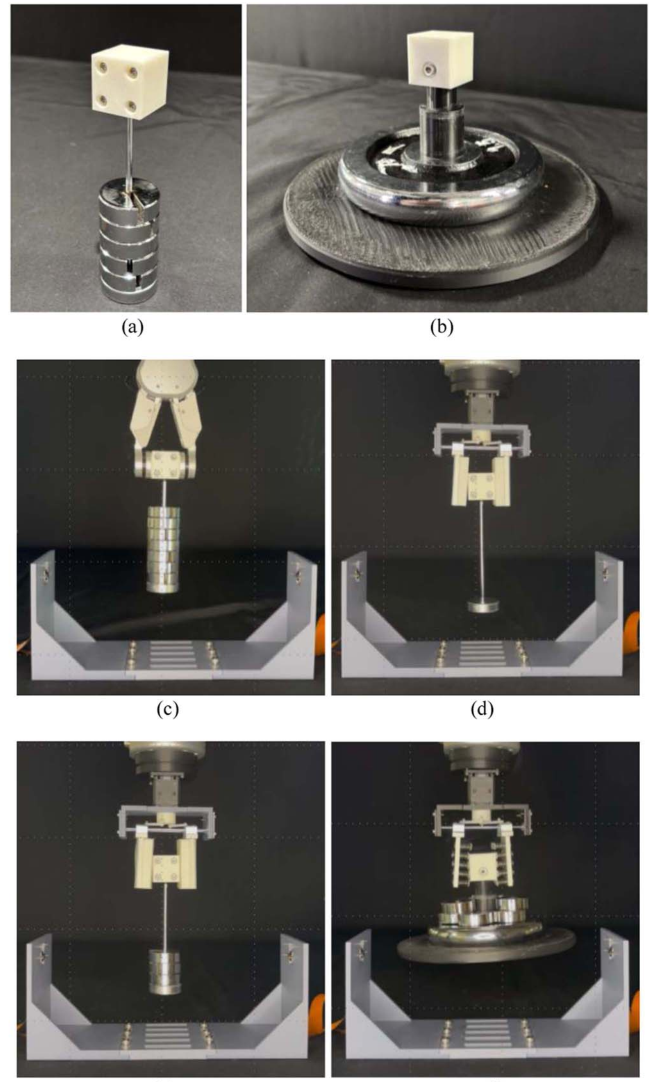

(a) (b) (c) (d) (e) (f)

Fig. 6. Experiment of payload measurement. (a) Test setup for low payload. (b) Test setup for high payload. (c) RG2-FT gripper. (d) Nonfrictional flat gripper. (e) Frictional flat gripper. (f) Proposed pin-array gripper.

The experimental results revealed significant differences in payload capacity among the tested grippers. The RG2-FT gripper [see Fig. 6(c)] successfully lifted up to 900 g but exhibited slippage, resulting in a stable maximum payload of 800 g. The nonfrictional flat gripper [see Fig. 6(d)] achieved a maximum lift of 100 g. The frictional flat gripper [see Fig. 6(e)] initially lifted 500 g but slipped during the test, yielding a final payload

TABLE I
COMPARISON OF GRASPING FORCE MEASUREMENT

Shape	RG2-FT Gripper	Flat Gripper with Fingertip	Pin-Array Gripper
Cylinder	6.96 N	3.14 N	8.13 N
Cube	8.53 N	1.76 N	6.96 N
Sphere	5.98 N	4.21 N	4.80 N
Tetrahedron	0.20 N	0.10 N	2.25 N
Stella Dodecahedron	5.98 N	5.98 N	6.86 N

capacity of 400 g. In contrast, the proposed pin-array gripper [see Fig. 6(f)] achieved a maximum stable lift of 2400 g without slippage. However, it failed to lift the 2500 g object due to insufficient gripping force to support the load. Importantly, no structural damage or pin failure was observed during the test.

The payload capacity of the pin-array gripper surpassed that of the RG2-FT, nonfrictional flat, and frictional flat grippers by factors of 3.00, 24.00, and 6.00, respectively. This superior performance is attributed to the unique pin-array design, which provides bottom-side mechanical support and a distributed pin structure that mitigates slippage and enables secure handling of heavier objects. Further enhancement of the payload capacity of the pin-array gripper may be achieved by employing a higher-torque gripping motor and optimizing the pin-array structure through metal-reinforced lower pins, enlarged pin radii, or a denser pin arrangement.

B. Grasping Force Measurement

Grasping force is also an important performance metric for a gripper, as it ensures secure handling of objects. An appropriate level of force is essential: excessive force may damage the object, whereas insufficient force can result in slippage due to limited friction.

To measure the grasping force, a piezoresistive force sensor (FlexiForce A201, Tekscan) was embedded inside the object being gripped, as shown in Fig. 7(a). The test objects—comprising a cylinder, cube, sphere, tetrahedron, and stellated dodecahedron—are shown in Fig. 7(b). Grasping force measurements were conducted using three different grippers: the RG2-FT gripper, the frictional flat gripper, and the proposed pin-array gripper. Note that the flat and pin-array grippers were driven by the same motor (Dynamixel XL-430, Robotis) to enable a fair comparison of the effect of surface geometry on grasping force under identical actuation conditions. Each experiment was performed three times under identical conditions to verify repeatability, and the average value was taken as the representative grasping force.

The results, summarized in Table I and illustrated in Fig. 7(c), indicate that the grasping forces of the RG2-FT gripper and the pin-array gripper followed similar trends for most grasp-friendly objects, with differences ranging from 0.80 to 1.17 times.

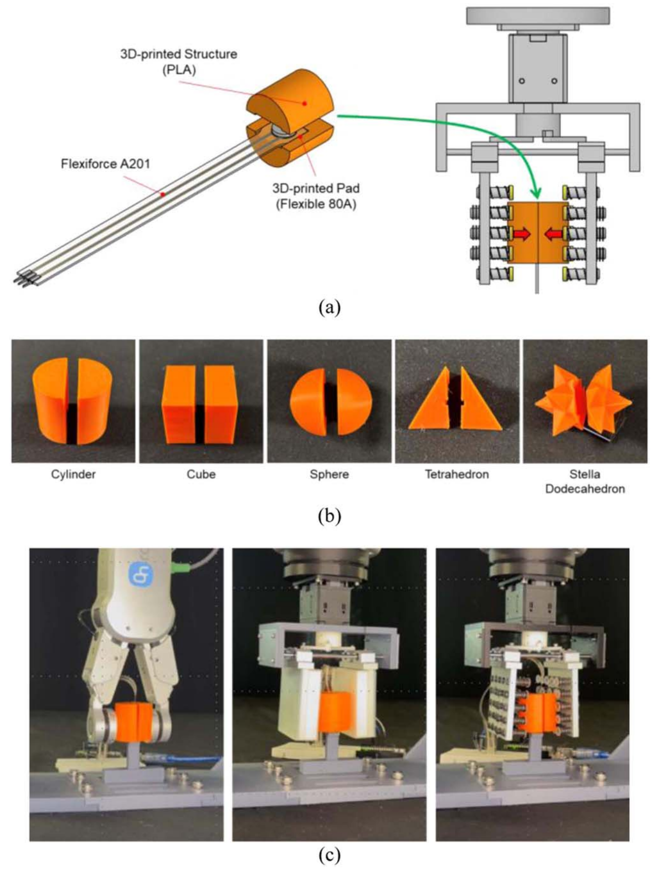

Fig. 7. Experiment of grasping force measurement. (a) Test setup. (b) Objects. (c) Experiment of RG2-FT, frictional flat, and pin-array gripper.

However, when handling geometrically challenging objects such as the tetrahedron, the RG2-FT gripper failed to maintain a stable grasp, resulting in slippage and preventing valid force measurements. This demonstrates that the pin-array gripper provides superior stability and is better suited for grasping irregularly shaped objects.

Although both the frictional flat gripper and the pin-array gripper were actuated by the same motor, the frictional flat gripper exhibited significantly weaker grasping forces. Depending on the object, the measured forces were between 1.14 and 23.00 times lower than those of the pin-array gripper. These findings highlight the robustness and reliability of the proposed pin-array gripper in achieving secure and stable grasps across a wide range of object geometries. Further enhancement of the grasping force capacity of the pin-array gripper may be achieved by employing a higher-torque gripping motor and optimizing the structural design of the pin-array, for example, by incorporating stiffer springs or increasing the density of parallel pins.

C. Dynamic Tool Manipulation

In this experiment, we introduce and evaluate a distinct performance metric for the gripper, emphasizing its capability to perform advanced tool-based manipulation tasks beyond conventional pick-and-place operations. Achieving better results in this metric requires stable payload handling, sufficient grasping

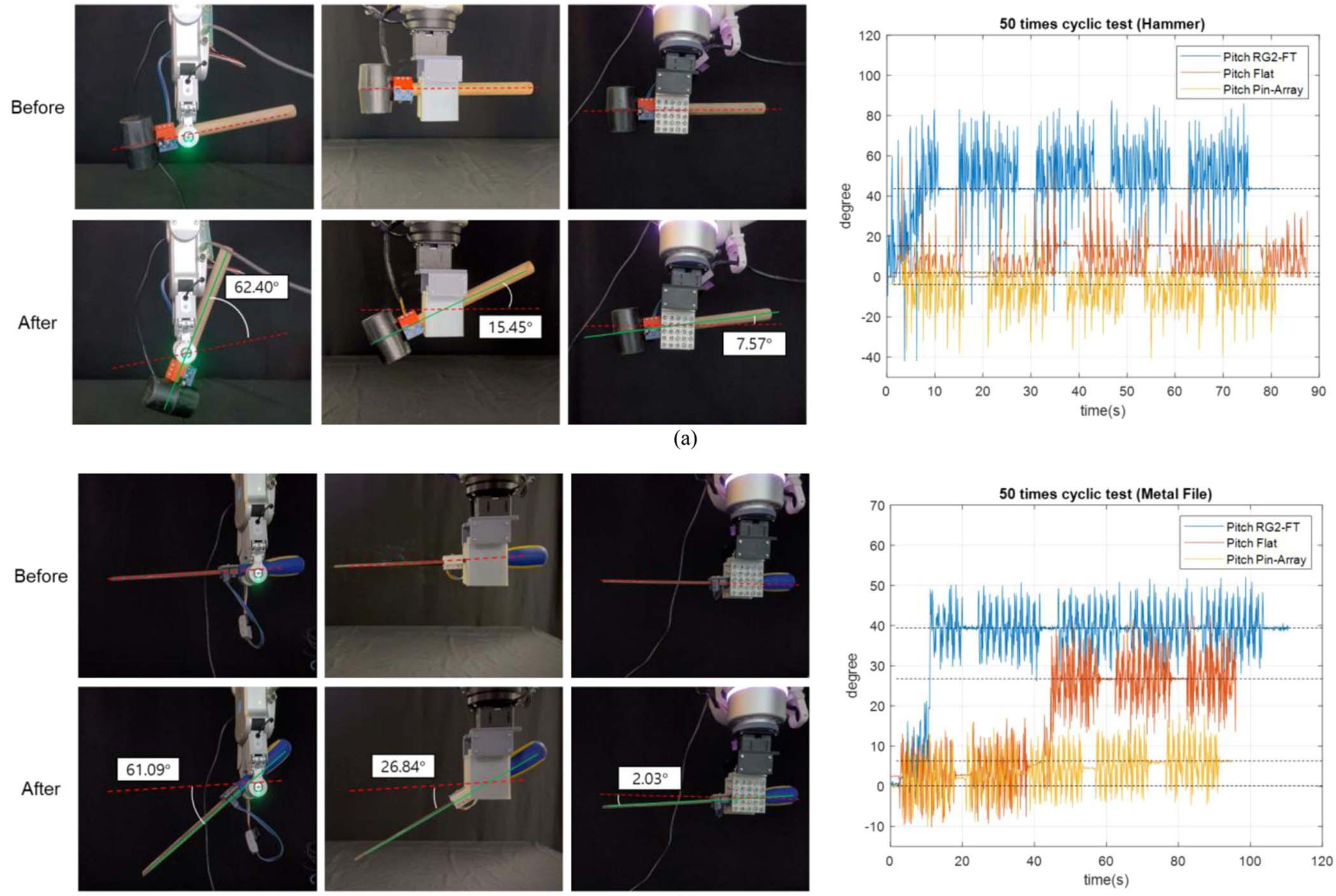

(b)

Fig. 8. Pitch angle deviations during tool manipulation tasks. (a) Hammer manipulation. (b) Metal file manipulation.

force, and adequate surface friction under dynamically changing tool conditions. This aligns with the original objective of developing the proposed pin-array gripper.

To quantify dynamic tool manipulation performance, we implemented the experimental setup described in Appendix A. An inertial measurement unit (IMU) sensor (MPU-9250) was attached to the tool to track changes in pitch angle before, during, and after the manipulation tasks, enabling the analysis of grasp stability and motion fidelity. Two tool manipulation scenarios were tested using a hammer and a metal file. Each tool demands distinct motion characteristics: the hammer requires a swinging motion (pitch-direction rotation), while the metal file involves linear filing motions (horizontal-direction translation). The experiment consisted of 50 operations, organized into 5 cycles of 10 repetitions each, to observe pitch angle variations over time. Three grippers were tested for comparison: the RG2-FT gripper, a frictional flat gripper, and the pin-array gripper.

In the case of the hammer, shown in Fig. 8(a), the RG2-FT gripper exhibited a pitch angle error of 43.56°, the flat gripper showed a pitch angle error of 15.45°, while the pin-array gripper showed a reduced pitch angle error of 2.01°. As the majority of the hammer's weight is concentrated at the head, both the RG2-FT and flat gripper tended to tilt forward, lacking sufficient support against gravity. The RG2-FT gripper exhibited an initial tilt during the first cycle, which then persisted across subsequent cycles. Similarly, the frictional flat gripper showed a tilt beginning in the second cycle, followed by a sustained tilted state. Although the pin-array gripper exhibited a slight initial tilt, its pitch angle deviation was 21.67 times smaller than that of the RG2-FT gripper and 7.69 times smaller than that of the flat gripper, indicating substantially improved stability.

For the metal file [see Fig. 8(b)], similar trends were observed. Although the filing motion is primarily horizontal and prismatic, the mass of the metal file is concentrated at the front, causing it to tilt forward due to insufficient support against gravity. The RG2-FT gripper exhibited a pitch angle error of 39.75°, the frictional flat gripper showed a pitch angle error of 26.84°, while the pin-array gripper maintained a significantly lower deviation of 6.03°. The pitch angle error of the pin-array gripper was reduced by factors of 6.59 and 4.45 compared to the RG2-FT and flat grippers, respectively, demonstrating superior repeatability and stability.

Further enhancement of the dynamic tool manipulation capacity of the pin-array gripper may be achieved by optimizing its structural design to better match the geometry of specific tools. This can be accomplished by adjusting the size and shape of individual pins, modifying the overall array configuration, or increasing the pin density.

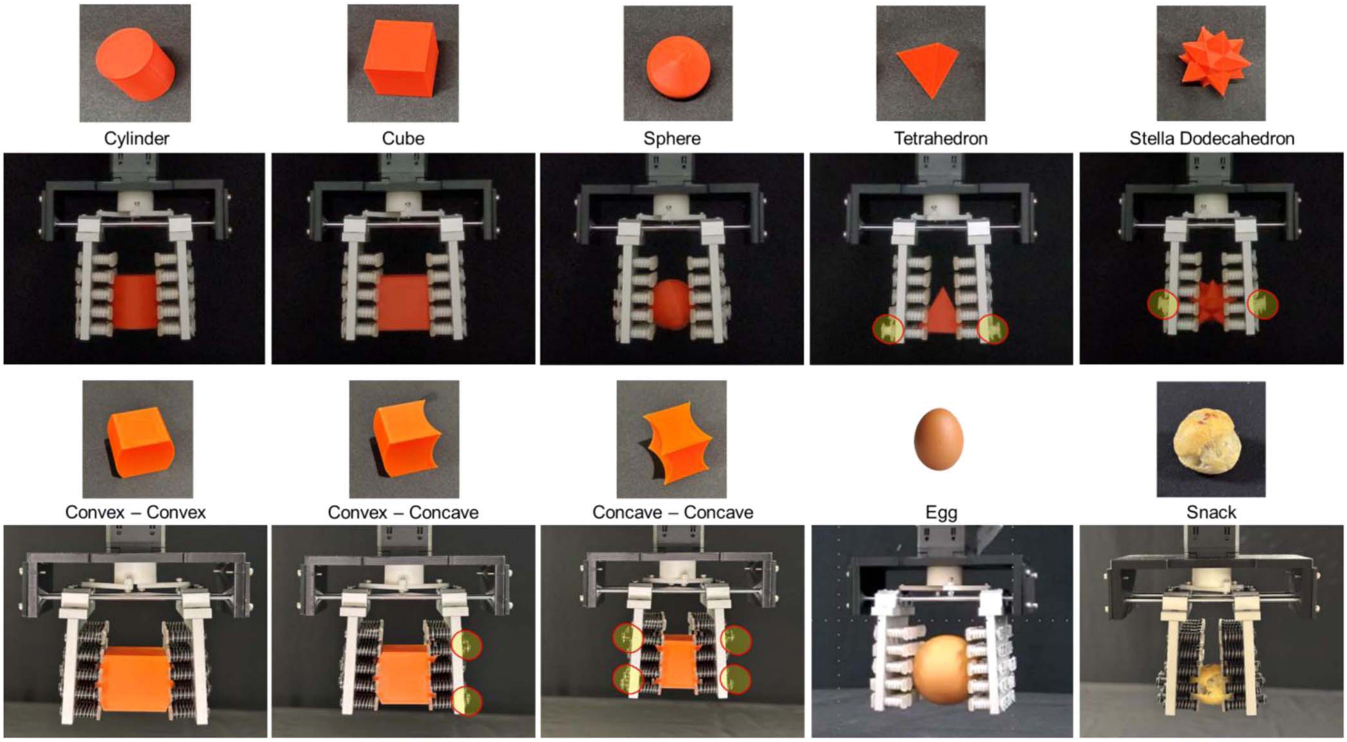

Fig. 9. Various shaped objects printed by a 3D printer, cylinder, cube, sphere, tetrahedron, stella doecahedron, convex-convex, convex-concave, concave-concave, egg, and snack.

VI. Practical Demonstrations

This section presents practical demonstrations of the pin-array gripper capabilities, including universal gripping, omnidirectional tool manipulation, tool usage, and its application in the mobile manipulator (LeeAhn2), providing a qualitative evaluation of its effectiveness in real-world tasks. The demonstration was performed solely with the pin-array gripper.

A. *Universal Gripping*

Universal gripping refers to the fundamental function of a conventional gripper, specifically for pick-and-place tasks, allowing it to handle objects of a certain size within its workspace [7], [34], [35]. Universal gripping performance is evaluated based on the ability to handle objects of various shapes commonly encountered in the environment, with effectiveness increasing as it accommodates a larger variety of objects. The experimental setup is described in Appendix A. The universal gripping experiment was conducted to grasp a set of commonly used N objects, as detailed in Appendix B.

The universal gripping experiment with eight 3D printed PLA plastic object shapes is shown in Fig. 9. This experiment aimed to verify the gripper's adaptability in effectively handling objects of various shapes. Ten objects with distinct shapes, each approximately 30 mm to fit within the gripper's workspace, were prepared: a cylinder, cube, sphere, tetrahedron, stellated dodecahedron, convex-convex, convex-concave, concave-concave, egg, and snack. All the objects were successfully gripped as shown in Fig. 9; however, the tetrahedron-shaped object proved challenging to grip effectively without friction-enhancing fingertip attachments, as tapered shapes often lead to slippage during gripping. This highlights the importance of frictional fingertips in enhancing grip stability when handling objects with sharp or slanted geometries.

The universal gripping experiment was conducted using common tools typically found in various settings, such as factories, homes, and offices. This approach evaluates the practicality of the gripper in handling objects with varied shapes, sizes, and material properties, showcasing its potential for versatile applications across diverse environments. Successfully grasping 68 out of a total of 71 objects, the gripper achieved a 95.7% success rate.

B. *Omnidirectional Tool Gripping*

Tools often require a specific orientation for effective use, making the way they are held essential [36], [37]. Omnidirectional gripping is a valuable capability for manipulators, and the pin-array gripper excels at securely grasping objects regardless of orientation. To verify this capability, we conducted experiments testing the ability to hold a screwdriver in three orientations: 1) horizontal (0°), 2) tilted at 45°, and 3) vertical (90°).

The results of omnidirectional tool gripping for a horizontally oriented screwdriver are shown in Fig. 10(a). A close-up of the pin-array section shows that the five central horizontal pins in the third row are aligned with the surface geometry of the screwdriver. The results of omnidirectional tool gripping for a 45° oriented screwdriver are shown in Fig. 10(b). A close-up of the pin-array section reveals that several diagonal central pins are aligned with the surface geometry of the screwdriver. The

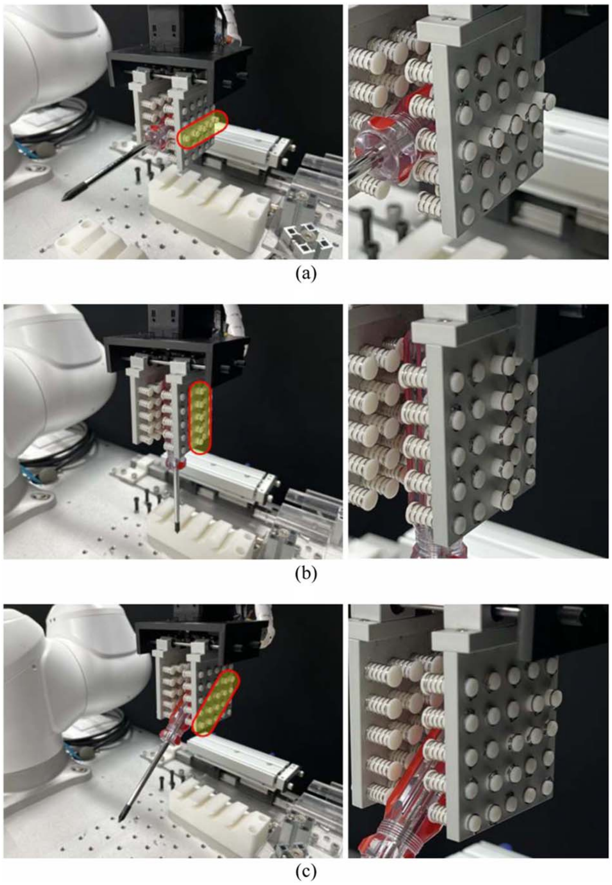

Fig. 10. Omnidirectional tool gripping at different orientations. (a) Horizontally oriented. (b) 45° tilted. (c) Vertically oriented.

results of omnidirectional tool gripping for a vertically oriented screwdriver are shown in Fig. 10(c). A close-up of the pin-array section reveals that several diagonal central pins are aligned with the surface geometry of the screwdriver. A close-up of the pin-array section shows that the five central vertical pins in the third column are aligned with the surface geometry of the screwdriver. The pressed pins are subjected to axial forces, while the unpressed pins adjacent to them experience bending forces. This grip configuration enhances stability and handling during tool manipulation, minimizing deviations in tilt and movement.

This experiment demonstrates the capability for omnidirectional tool gripping, enabling the gripper to effectively grasp and hold objects regardless of their orientation. While only three orientations are shown, the gripper can operate in any direction, highlighting its suitability for various applications where object orientations may vary in real-world industrial environments.

C. Tool Usage

This section demonstrates the gripper's ability to handle objects outside its specified range using external tools, inspired by human use of tools to manage objects of varying sizes. The study illustrates the gripper's performance in manipulating objects both smaller and larger than its conventional gripping workspace (10–47 mm).

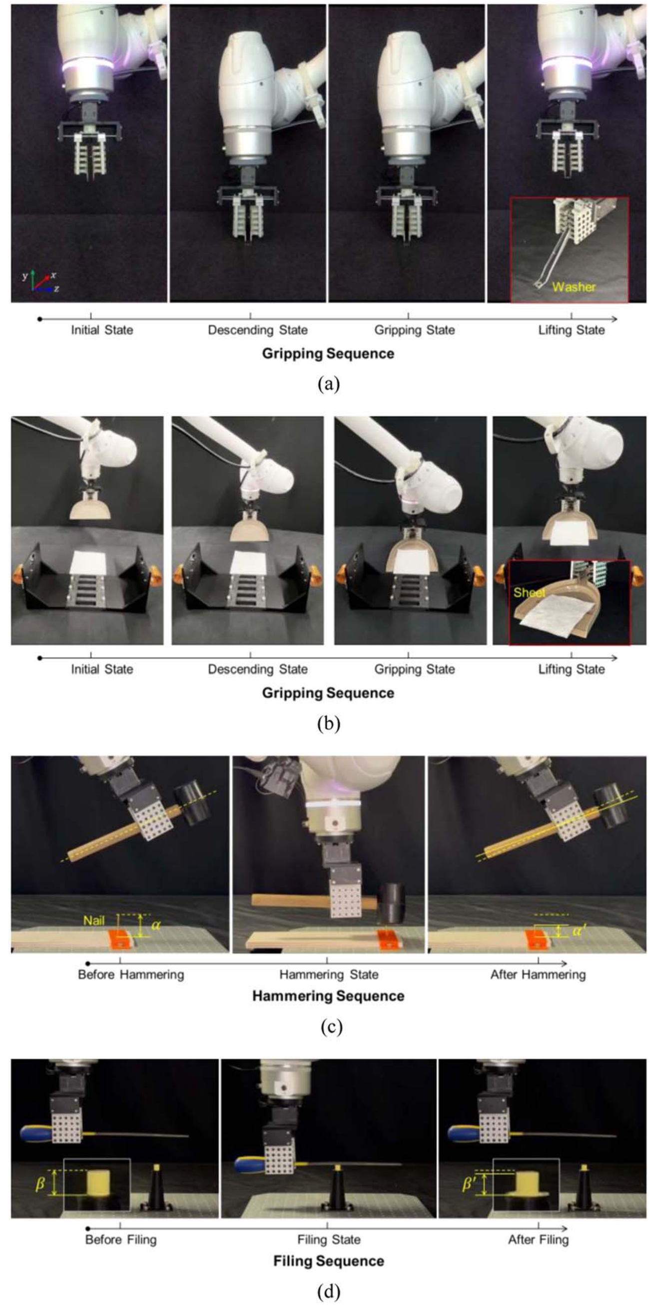

Fig. 11. Demonstration of tool usage. (a) Tweezer for gripping small objects. (b) Dustpan for gripping large objects. (c) Hammer for nail-driving. (d) Metal file for chalk-abrasion.

Tool usage demonstrations are divided into two categories: 1) objects smaller than the gripping workspace (less than 10 mm) and 2) objects larger than the gripping workspace (more than 47 mm). For objects smaller than the workspace, as shown in Fig. 11(a), the gripper uses tools such as tweezers. For example, a small washer with a diameter of 8 mm, thickness of 1 mm, and weight of 0.14 g was successfully picked up using tweezers. For objects larger than the workspace, as shown in Fig. 11(b), the gripper uses tools like a dustpan. A napkin, with dimensions of 120 mm × 120 mm (approximately 2.4 times larger than the size of the existing gripping workspace), a thickness of 0.3 mm, and

TABLE II
EXPERIMENTAL SETUP FOR TOOL USAGE

Category		Hammer	Metal File
Task		Nail-driving	Chalk-abrasion
Workpiece		Balsa wood sheets Nail 3D-printed jig	Chalk 3D-printed jig
Tool		Hammer	Metal file
Robot Path	Kinematics	J5: 20° + J3: 9°	100 mm stroke
	Dynamics	80 deg·s⁻¹ 550 deg·s⁻²	130 mm·s⁻¹ 1 mm·s⁻²
	Contact	1 mm below nail head	0.5 mm below chalk
	Cycle	10 strikes per trial	10 strokes per trial
Test Trials		3	3
Evaluation Metrics		Nail penetration depth	Chalk-abrasion depth

a weight of 1.0 g, was lifted using the dustpan. These examples demonstrate the gripper's versatility in handling objects beyond its typical range using tools.

In addition, the gripper's ability to manipulate tools like a hammer and a metal file was demonstrated. Fig. 11(c) illustrates the gripper's application in hammer usage, showing its ability to securely handle the hammer for effective manipulation. The hammering experiment is designed to perform a nail-driving task. The setup consisted of six stacked balsa wood sheets (1 mm thickness each; total 6 mm), with a wood nail (diameter 2 mm, head diameter 5 mm, length 40 mm) fixed in a custom 3D-printed jig. The 6 mm balsa stack was placed on a 10.5 mm aluminum plate with a recessed pocket, providing an underlying air gap that allowed the nail to penetrate the wood without contacting the metal substrate. The hammer comprised a cylindrical rubber head (diameter 44 mm and length 71 mm) and a wooden handle (diameter 18 mm and length 200 mm), with a total mass of 230.15 g. To maintain normal hammer–nail contact within the collaborative robot's kinematic constraints, a swing path was planned such that joint 5 and joint 3 executed synchronous rotations of 20° and 9°, respectively, generating auxiliary vertical motion and an up–down striking action. The two joints' rotational velocity and acceleration were set to 80 and 550 deg·s^{-2}. During the downswing, the gripper's lowest point was positioned approximately 1 mm below the nail head to ensure that the impact was transmitted to the nail. Each trial comprised 10 strikes; three trials were conducted, yielding nail penetration depths $\Delta\alpha = \alpha - \alpha'$ of 15, 16, and 14 mm (mean = 15 mm). A concise summary of the experimental setup is provided in Table II. Fig. 11(d) presents the use of the metal file, where the gripper demonstrated stable and precise control for performing tasks requiring tool manipulation. The filing test is designed to perform a chalk-abrasion task. A cylindrical chalk specimen (diameter 10 mm and length 81 mm) was secured in a custom 3D-printed jig whose internal diameter was 10.3 mm, providing a 0.3 mm clearance. The metal file (length 310 mm, mean width

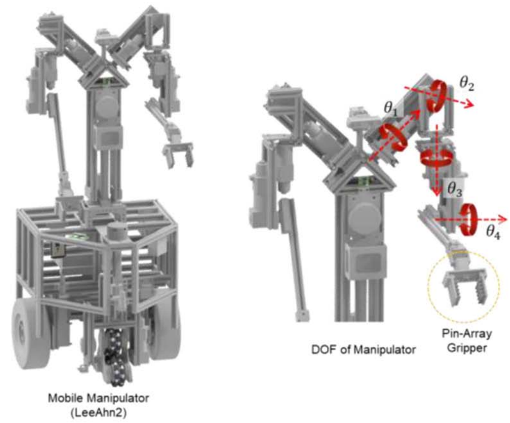

(a)

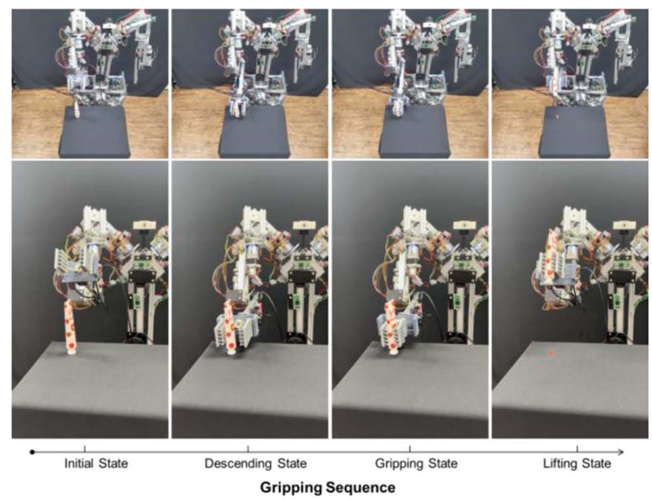

(b)

Fig. 12. Application in mobile manipulator. (a) Overview of LeeAhn2. (b) Grasping application.

20 mm, mass 173.15 g, grade 2 cut for medium coarseness) was actuated by a collaborative robot. To maintain near-horizontal tool–workpiece contact within the robot's kinematic constraints, a stroke path was planned with a linear velocity of 130 mm s^{-1} and a linear acceleration of 1 mm s^{-2}. The stroke height was set 0.5 mm below the chalk surface to ensure effective engagement, and each trial executed 10 reciprocating strokes over a 100 mm path. Three trials were conducted, yielding chalk-abrasion depths $\Delta\beta = \beta - \beta'$ of 1.0, 1.5, and 1.5 mm (mean = 1.3 mm). A concise summary of the experimental setup is provided in Table II. For evaluation, we defined the success criterion of hammer usage as achieving a cumulative nail penetration depth greater than 15 ± 1 mm after 10 strikes, while maintaining stable tool retention and without excessive off-axis misalignment. Trials not meeting these conditions were regarded as failures. These tests highlight the gripper's dual functionality: not only can it grasp tools, but it can also use them for specific tasks.

The figures and results provide a clear depiction of the gripper's expanded range of operation with tools, reinforcing its adaptability for a wide range of applications.

D. Pin-Array Gripper in Mobile Manipulator

The mobile manipulator LeeAhn2, depicted in Fig. 12(a), consists of a wheel-based mobile platform and a dual-arm manipulator mounted on a torso structure. Each arm offers four degrees of freedom (DOF), which is lower than the 7-DOF found in a human arm, where the shoulder provides 3-DOF, the elbow 1-DOF, and the wrist 3-DOF. This limited DOF means that, without additional flexibility, the manipulator's movements in Cartesian space can be restricted, especially in tasks requiring universal gripping and complex orientations. However, by integrating a pin-array gripper, LeeAhn2 compensates for these limitations, gaining enhanced adaptability and stability for gripping tasks. The pin-array structure allows it to conform to various object shapes, making it especially suitable for diverse handling requirements. Fig. 12(b) illustrates an experiment where LeeAhn2, equipped with the pin-array gripper, successfully picks up an object in practical scenarios.

VII. Conclusion

This study developed a novel frictional and prismatic pin-array gripper, developed to overcome the limitations of traditional grippers in universal gripping and tool manipulation. The gripper's adaptable pin-array structure offers an expanded contact point and nonslip frictional fingertips, ensuring stable handling across various shapes and surfaces. With an omnidirectional, spring-actuated pin design, the gripper enables omnidirectional gripping and performs effectively in unstructured environments. Experimental results demonstrated the superior performance of the pin-array gripper over conventional grippers, handling a broader range of objects with enhanced stability in tool manipulation tasks. The gripper was successfully applied to both a conventional industrial manipulator and the mobile manipulator LeeAhn2, showcasing its versatility for automation in diverse settings.

Future research will explore several key areas. Three potential topics for future work include:

1) expanding the use of robots for diverse and practical tool manipulation tasks;
2) conducting structural and mechanical optimization of various parametric pin-array grippers;
3) performing fatigue analysis, including accelerated life cycle testing and usage-frequency mapping to enhance durability and performance.

Appendix A
Experimental Test-Bed and Setup

The overall system and experimental setup are shown in Fig. 13(a). The hardware configuration includes a pin-array gripper mounted on a Doosan M1013 collaborative robot, actuated by a Dynamixel XL-430 motor connected to the host PC via a U2D2 power hub board. An MPU 9250 IMU sensor is attached to the tool during object and tool grasping to monitor holding stability. The system is divided into control and monitoring parts.

In the control part, motion control directs the gripper along a specified path. When a path command is issued, the collaborative robot follows the path in a single direction. The host PC initiates gripping control by sending grasp or release commands, which are processed by the control function and transmitted to the XL-430 motor. The motor's status (angle and load) is then relayed back to the host PC. If the motor reaches its rotation limit or the load exceeds a preset threshold, it stops automatically.

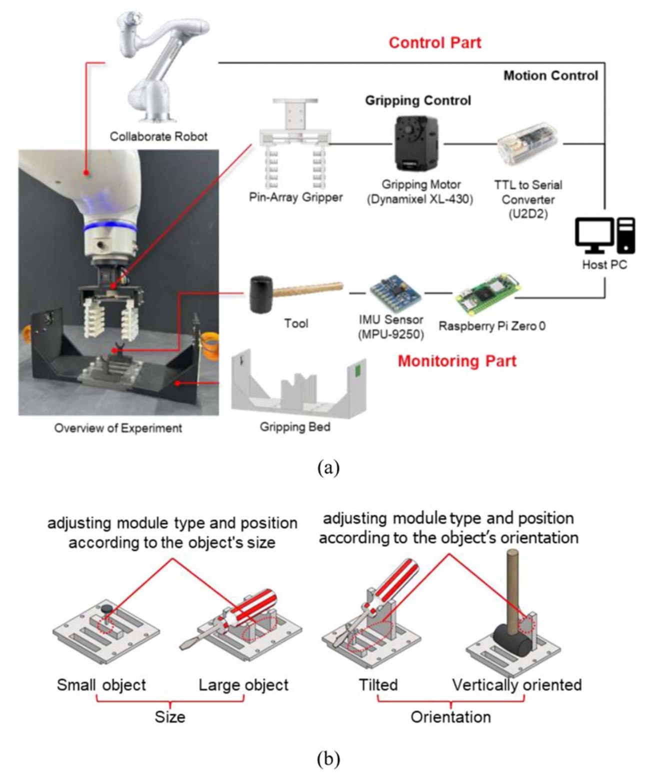

Fig. 13. Experiment Setup. (a) System Overview. (b) Detail of gripping bed and modules.

Fig. 13(b) shows the structure of the gripping bed used for pick-and-place experiments. For objects on the floor, the gripper uses only the pins at the end of the array plate. To accommodate different positions and orientations, a modular gripping bed with a central tool holder was designed. The tool holder is adjustable, allowing modules to be inserted at desired positions. This flexibility enables the gripping bed to adapt to various object sizes and orientations.

Appendix B
N Object Set

The set used in this experiment includes 71 diverse items commonly found in various environments, such as laboratories, workshops, offices, and homes. Measurement tools include a (1) scraper, (2) vernier calipers, (3) tape measure, (4) ruler, (5) micrometer, and (6) weight. General-purpose items include an (7) aluminum profile, (8) clock, (9) dustpan, (10) brush, (11) whisk, (12) scissors, and (13) magnets. Electronics and office supplies include a (14) charger, (15) Bluetooth earphone, (16) calculator, (17) USB hub, (18) mouse, and (19) flashlight, along with (20) sticky notes, a (21) stapler, (22) eraser, (23) batteries, (24) ink, (25) paperclips, and (26) push pins. Workshop tools encompass a (27) soldering iron, (28) rubber mallet, (29) screwdriver, (30) wrench, (31) drive socket, (32) desoldering tool, (33) tweezer, (34) metal file, (35) syringe, and (36) diagonal plier, (37) stir bar as well as various fastening items like (38) nails, (39) bolts, (40) nuts, (41) washer, and (42) springs. Additional items include a (43) knife, (44) spoon, (45) napkin, (46) door stopper, (47) drill, (48) toothbrush, (49) glass bottle, (50) petri dish, (51) wire, (52) lab tape, (53) sandpaper, (54) cleaning pill, and (55) glue. Recreational and everyday items such as (56) toothpaste, a (57) doll, (58) Couque D'asse (a snack), (59) jelly, (60) boiled egg, (61) hand cream, (62) spray bottle, and (63) ping pong ball, as well as lab-specific items like (64) SLA printing and (65) 3D printing components, are also included. This selection demonstrates the gripper's versatility in handling objects with varied shapes, sizes, and material properties. Additionally, the set of demonstration objects was later expanded to include an (66) egg, a (67) snack, (68) glass bottle 1, (69) glass bottle 2, a (70) small figurine, and a (71) Vaseline jar.

References

[1] Z. Hu, W. Wan, and K. Harada, "Designing a mechanical tool for robots with two-finger parallel grippers," *IEEE Robot. Automat. Lett.*, vol. 4, no. 3, pp. 2981–2988, Jul. 2019.

[2] Z. Hu, W. Wan, K. Koyama, and K. Harada, "A mechanical screwing tool for parallel grippers—Design, optimization, and manipulation policies," *IEEE Trans. Robot.*, vol. 38, no. 2, pp. 1139–1159, Apr. 2022.

[3] H.-S. Kim and G.-S. Kim, "Development of an intelligent gripper that determines the gripping force according to the weight of the object," *Int. J. Precis. Eng. Manuf.*, vol. 24, no. 12, pp. 2259–2268, 2023.

[4] M. Shaqura and J. S. Shamma, "A novel gripper design for multi-hand tools grasping under tight clearance constraints and external torque effect," in *Proc. IEEE Int. Conf. Mechatron. Automat.*, 2017, pp. 840–845.

[5] W. Wang, C. Li, M. Cho, and S.-H. Ahn, "Soft tendril-inspired grippers: Shape morphing of programmable polymer–paper bilayer composites," *ACS Appl. Mater. Interfaces*, vol. 10, no. 12, pp. 10419–10427, 2018.

[6] F. Ilievski, A. D. Mazzeo, R. F. Shepherd, X. Chen, and G. M. Whitesides, "Soft robotics for chemists," *Angew. Chem. Int. Ed.*, vol. 50, no. 8, pp. 1890–1895, 2011.

[7] J. R. Amend, E. Brown, N. Rodenberg, H. M. Jaeger, and H. Lipson, "A positive pressure universal gripper based on the jamming of granular material," *IEEE Trans. Robot.*, vol. 28, no. 2, pp. 341–350, Apr. 2012.

[8] W. Wang, H. Rodrigue, H.-I. Kim, M.-W. Han, and S.-H. Ahn, "Soft composite hinge actuator and application to compliant robotic gripper," *Composites Part B, Eng.*, vol. 98, pp. 397–405, 2016.

[9] P. Glick, S. A. Suresh, D. Ruffatto, M. Cutkosky, M. T. Tolley, and A. Parness, "A soft robotic gripper with gecko-inspired adhesive," *IEEE Robot. Automat. Lett.*, vol. 3, no. 2, pp. 903–910, Apr. 2018.

[10] T. Wu, Z. Liu, B. Wang, Z. Ma, D. Ma, and X. Deng, "A versatile topology-optimized compliant actuator for soft robotic gripper and walking robot," *Soft Robot.*, vol. 11, no. 1, pp. 157–170, 2024.

[11] W. G. Bircher, A. M. Dollar, and N. Rojas, "A two-fingered robot gripper with large object reorientation range," in *Proc. IEEE Int. Conf. Robot. Automat.*, 2017, pp. 3453–3460.

[12] Y. Cui, X. An, Z. Lin, Z. Guo, X.-J. Liu, and H. Zhao, "Design and implementation of an underactuated gripper with enhanced shape adaptability and lateral stiffness through semi-active multi-degree-of-freedom endoskeletons," *Int. J. Robot. Res.*, vol. 43, no. 6, pp. 873–896, 2024.

[13] A. Mo and W. Zhang, "A novel universal gripper based on meshed pin-array," *Int. J. Adv. Robot. Syst.*, vol. 16, no. 2, 2019, Art. no. 1729881419834781.

[14] B.-J. Yi et al., "Design of a parallel-type gripper mechanism," *Int. J. Robot. Res.*, vol. 21, no. 7, pp. 661–676, 2002.

[15] H. Fu, H. Yang, W. Song, and W. Zhang, "CTSA hand: A novel cluster-tube self-adaptive robot hand," in *Proc. IEEE Int. Conf. Robot. Biomimetics*, 2017, pp. 442–448.

[16] P. B. Scott, "The 'Omnigripper': A form of robot universal gripper," *Robotica*, vol. 3, no. 3, pp. 153–158, 1985.

[17] W. Hasan, L. Gerez, and M. Liarokapis, "Model-free, vision-based object identification and contact force estimation with a hyper-adaptive robotic gripper," in *Proc. IEEE Int. Conf. Mechatron. Automat.*, 2020, pp. 9514–9520.

[18] T. Feix, I. M. Bullock, and A. M. Dollar, "Analysis of human grasping behavior: Object characteristics and grasp type," *IEEE Trans. Haptics*, vol. 7, no. 3, pp. 311–323, Jul.–Sep. 2014.

[19] G. Bai, X. Kong, and J. M. Ritchie, "Kinematic analysis and dimensional synthesis of a meso-gripper," *J. Mech. Robot.*, vol. 9, no. 3, 2017, Art. no. 031017.

[20] K. Harada et al., "Proposal of a shape adaptive gripper for robotic assembly tasks," *Adv. Robot.*, vol. 30, no. 17/18, pp. 1186–1198, 2016.

[21] Y.-J. Kim, H. Song, and C.-Y. Maeng, "BLT gripper: An adaptive gripper with active transition capability between precise pinch and compliant grasp," *IEEE Robot. Automat. Lett.*, vol. 5, no. 4, pp. 5518–5525, Oct. 2020.

[22] Q. Lu, A. B. Clark, M. Shen, and N. Rojas, "An origami-inspired variable friction surface for increasing the dexterity of robotic grippers," *IEEE Robot. Automat. Lett.*, vol. 5, no. 2, pp. 2538–2545, Apr. 2020.

[23] M. R. Cutkosky and P. K. Wright, "Friction, stability, and the design of robotic fingers," *Int. J. Robot. Res.*, vol. 5, no. 4, pp. 20–37, 1986.

[24] M. Guo et al., "Design of parallel-jaw gripper tip surfaces for robust grasping," in *Proc. IEEE Int. Conf. Robot. Automat.*, 2017, pp. 2831–2838.

[25] F. Wan, H. Wang, J. Wu, Y. Liu, S. Ge, and C. Song, "A reconfigurable design for omni-adaptive grasp learning," *IEEE Robot. Automat. Lett.*, vol. 5, no. 3, pp. 4210–4217, Jul. 2020.

[26] Q. Xia et al., "An omnidirectional encircled deployable polyhedral gripper for contactless delicate midwater creatures sampling," *Adv. Eng. Mater.*, vol. 25, no. 8, 2023, Art. no. 2201416.

[27] A. Parness et al., "Gravity-independent rock-climbing robot and a sample acquisition tool with microspine grippers," *J. Field Robot.*, vol. 30, no. 6, pp. 897–915, 2013.

[28] C. V. Ince, J. Geggier, and A. Raatz, "Accuracy examination of a flexible pin gripper for forging applications," in *MHI Colloquium*. Berlin, Germany: Springer-Verlag, 2022, pp. 343–353.

[29] Z. Flintoff, B. Johnston, and M. Liarokapis, "Single-grasp, model-free object classification using a hyper-adaptive hand, google soli, and tactile sensors," in *Proc. IEEE/RSJ Int. Conf. Intell. Robots Syst.*, 2018, pp. 1943–1950.

[30] Y. Tanaka, Y. Shirai, Z. Lacey, X. Lin, J. Liu, and D. Hong, "An underactuated whippletree mechanism gripper based on multi-objective design optimization with auto-tuned weights," in *Proc. IEEE/RSJ Int. Conf. Intell. Robots Syst.*, 2021, pp. 6139–6146.

[31] K. Nagaoka et al., "Passive spine gripper for free-climbing robot in extreme terrain," *IEEE Robot. Automat. Lett.*, vol. 3, no. 3, pp. 1765–1770, Jul. 2018.

[32] T. Laliberte, L. Birglen, and C. Gosselin, "Underactuation in robotic grasping hands," *Mach. Intell. Robot. Control*, vol. 4, no. 3, pp. 1–11, 2002.

[33] B. Vanderborght, R. Van Ham, D. Lefeber, T. G. Sugar, and K. W. Hollander, "Comparison of mechanical design and energy consumption of adaptable, passive-compliant actuators," *Int. J. Robot. Res.*, vol. 28, no. 1, pp. 90–103, 2009.

[34] M.-S. Choi et al., "Development of multi-purpose universal gripper," in *Proc. IEEE Int. Conf. Mechatron. Automat.*, 2017, pp. 1421–1424.

[35] D. Sui et al., "A bioinspired soft swallowing gripper for universal adaptable grasping," *Soft Robot.*, vol. 9, no. 1, pp. 36–56, 2022.

[36] C. C. Kemp and A. Edsinger, "Robot manipulation of human tools: Autonomous detection and control of task-relevant features," in *Proc. 5th Int. Conf. Develop. Learn.*, 2006, vol. 42.

[37] A. Billard and D. Kragic, "Trends and challenges in robot manipulation," *Science*, vol. 364, no. 6446, 2019, Art. no. *eaat8414*.

Cheonghwa Lee received the B.S. and M.S. degrees in mechanical system engineering from the Kumoh National Institute of Technology, Gumi, South Korea, in 2017 and 2019, respectively, and the Ph.D. degree in electrical and computer engineering from Seoul National University, Seoul, South Korea, in 2025.

He was a postdoctoral researcher with the University of Connecticut, Storrs, CT, USA. He is currently an assistant professor with the School of Mechanical Engineering, Kumoh National Institute of Technology. His research interests include intelligent robotics and advanced manufacturing, with a focus on practical industrial deployment of robotic systems.

Hyeongwon Kim received the B.S. degree in mechanical engineering from Sogang University, Seoul, South Korea, in 2023, and the M.S. degree in mechanical engineering from Seoul National University, Seoul, in 2025. She is currently working toward the Ph.D. degree in mechanical engineering with Seoul National University, Seoul, South Korea.

Her research interests include physically adaptive robotic mechanisms, pin-array actuation, and soft–rigid hybrid robotics.

Midum Oh received the B.S. degree in mechanical engineering from Sogang University, Seoul, South Korea in 2022, the M.S. degree in mechanical engineering from Seoul National University, Seoul, in 2024.

Her research interest included sensors that are applicable to smart factory and robotics.

Kisu Ok received the B.S. and M.S. degrees in computer engineering from the Keimyung University, Deagu-si, Gyeongsangbuk-do, South Korea, in 2015 and 2016, respectively. He is currently working toward the Ph.D. degree in electrical and computer engineering with Seoul National University, Seoul, South Korea.

He was a researcher with the Korea Electronic Technology Institute, Seongnam-si, Gyeonggi-do, Korea. His current research interest focuses on artificial intelligence-based robotic automation control and applications.

Sung-Hoon Ahn received the Ph.D. degree in aerospace engineering, with a minor in mechanical engineering, from Stanford University, Stanford, CA, USA, in 1997.

He was a Postdoctoral Researcher and Lecturer with the University of California in Berkeley and an Assistant Professor with Gyeongsang National University. He is currently a full Professor with the Department of Mechanical Engineering, Seoul National University. His research interests include smart factories, sensors/actuators, appropriate technology, robotics, smart grids, 3-D/4-D printing, composite materials, and micro/nanofabrication.

Dr. Ahn is a fellow of CIRP (the International Academy for Production Engineers) and the Korean Academy for Science and Technology and an Associate Member of the National Academy of Engineers of Korea.